JOURNAL OF SOLID STATE CHEMISTRY **103**, 466–471 (1993)

A Tri-α-PbO_2 Related Structure: $Li_4ZnIn_2F_{12}$

J-J. MAGUER AND G. COURBION

Laboratoire des Fluorures, U.R.A. C.N.R.S. 449, Faculté des sciences, Université du Maine, 72017 Le Mans Cedex, France

Received July 17, 1992; in revised form September 21, 1992; accepted September 22, 1992

The compound $Li_4ZnIn_2F_{12}$ has been synthesized in the form of single crystals. The symmetry of the unit cell is orthorhombic: $a = 4.7465(6)$ Å, $b = 17.592(2)$ Å, $c = 5.0582(6)$ Å, with space group *Pbcn*, $Z = 2$. The structure has been determined using 525 independent reflections ($R = 0.015$, $R_w = 0.018$). This phase exhibits a new cationic distribution inside an h.c. packing of F^- ions; four cationic sites are occupied, two of them being statistically filled (zinc and lithium at one and half a lithium at the other). The stacking of octahedra is strongly related to the tri-α-PbO_2 structure. An isotypic $Li_4MIn_2F_{12}$ series with M = Mg, Fe, Co, Ni is evidenced. © 1993 Academic Press, Inc.

Introduction

$AMM'F_6$ ternary fluorides (A = Li, Na; M^{2+} and M^{3+} = 3*d* transition cations or Al, Ga, In) mainly adopt two structural types: trirutile (*1–5*) or Na_2SiF_6 (*6–9*). In some cases, a dimorphism is observed between these two types either by increasing the pressure ($LiFe_2F_6$ (*10*) and $LiMTiF_6$ (*11*)) or by heating and quenching ($LiMnVF_6$ (*12*)). In each case, the Na_2SiF_6-type is the most dense. Dimorphism is also observed within the Na_2SiF_6-type for the compound $LiMnFeF_6$ (*8*); the structural difference between the two phases is mainly due to an inversion between alkali and trivalent Fe^{3+} ions.

These structures consist of different cationic distributions in half of the octahedral sites of a pseudo-h.c. packing of F^- ions. It can be noted that with O^{2-} ions in the same packing, AB_2O_6 oxides easily crystallize with columbite (*13*) or tri-α-PbO_2 (*14*) structures.

$LiMInF_6$ compounds (*9*) belong to the Na_2SiF_6-type with a cationic distribution close to that of α-$LiMnFeF_6$, but no dimorphism is reported. Our investigation of the ternary system LiF–ZnF_2–InF_3, by both solid state reaction and crystal growth in chloride flux, evidenced a new orthorhombic phase, the molar volume of which is very close to that of $LiZnInF_6$. This led us to determine the structure of this new compound, whose formula was found to be $Li_4ZnIn_2F_{12}$.

This paper deals with the crystal structure of this new phase and the characterization of an isotypic series.

Experimental

Preparation

Crystals of $Li_4ZnIn_2F_{12}$ were obtained by using a chloride flux method (*15, 16*) in a platinum crucible under argon atmosphere. A stoichiometric mixture of the elementary

0022-4596/93 $5.00

TABLE I

CRYSTAL DATA AND CONDITIONS OF DATA COLLECTION AND REFINEMENT FOR $Li_4ZnIn_2F_{12}$

Symmetry	orthorhombic
Space group	*Pbcn* (No. 60)
Z	2
Parameters	
a	4.7496(5) Å
b	17.606(2) Å
c	5.0617(6) Å
Volume	423.3(2) Å^3
Calculated density	4.32
Crystal size	3.5 10^{-4} mm^3
Reflections used to refine cell parameters	32
Scan mode ω-2Θ in N steps of $\Delta\omega = 0.035$	$37 \leq N \leq 43$
Data collection range	$2\Theta \leq 70°$
Aperture	3.5 × 3.5 mm
Standard reflections	$-2, 6, 1$ $-2, -6, -1$ $-2, 0, -2$
Measured reflections	2226
Min and max h, k, l	$-7, -20, -6; 7, 28, 8$
Independent reflections ($I > 3\sigma(I)$)	525
R (from averaging)	0.019
Absorption	$\mu = 84.0$ cm^{-1}
Secondary extinction factor	$\varepsilon = 2.6(4)\ 10^{-7}$
Weighting scheme	$W = 0.61/(\sigma^2(F) + 0.0014F^2)$
Number of refined parameters	43
Max, min heights in the final difference map	$+1.3, -0.6$ e Å^{-3}
Reliability factors R; R_w	0.015; 0.018

fluorides was not necessary to give single crystals of this phase. In fact, the best results were obtained from the mixture $2LiF + ZnF_2 + InF_3 + 8ZnCl_2$, by slow cooling (5°C/h) from 500°C. Beside $Li_4ZnIn_2F_{12}$ crystals in form of platelets, some hexagonal or trigonal prisms of $LiZnInF_6$ were found together with small amounts of Li_3InF_6. Thermal study (DTA Netzsch 404 S, heating rate 300°C/hr) of $Li_4ZnIn_2F_{12}$ only showed an endothermic peak at 580(5)°C corresponding to the melting point; no transition peak indicating the formation of the $LiZnInF_6$ phase was observed (M.P. = 625(5)°C for $LiZnInF_6$). The solid state synthesis of $Li_4ZnIn_2F_{12}$ was achieved in sealed gold tubes at 575°C (16 hr) from a stoichiometric mixture of the elementary fluorides. In the same conditions an isotypic series was synthesized with $M^{II} = Mg^{2+}$, Co^{2+}, Ni^{2+}, Fe^{2+}, but failed with Mn^{2+}. Attempts to substitute 3*d* trivalent cations for In^{3+} led to a mixture of $LiMM'F_6$ and $Li_3M'F_6$ phases ($M = Co^{2+}$, Ni^{2+}, and $M' = Cr^{3+}$, Fe^{3+}).

X-Ray Data Collection and Characterization

The crystal selected for X-ray data collection on a SIEMENS AED2 four-circle diffractometer (Mo*Kα*) was limited by faces $\pm\{010, \bar{2}03, 101\}$. The conditions of the diffraction experiment are given in Table I. The lattice parameters —$a = 4.7496(5)$ Å, $b = 17.606(2)$ Å, $c = 5.0617(6)$ Å—were refined from 32 reflections ($2\Theta \approx 30°$), centered by the double scan technique. The observed limiting conditions for the reflections—$0kl$, $l = 2n$; $h0l$, $l = 2n$; and $hk0$, $h + k = 2n$—were consistent with the *Pbcn* space group. The X-ray powder diffraction patterns of the isotypic series were indexed with an orthorhombic lattice, whose refined cell parameters are given in Table II. This table also allows a comparison of the unit cell volumes of the $Li_4MIn_2F_{12}$ phases with the hexagonal cell of $LiZnInF_6$. In spite of the differences in lattice symmetry, the similarities in observed volumes indicate that the structures of these species probably are based on the same anionic packing.

Structure Determination

All the calculations were performed using the SHELX-76 (*17*) and SHELS-86 (*18*) pro-

TABLE II

CELL PARAMETERS[a] (Å) OF $Li_4MIn_2F_{12}$

	a	*b*	*c*	V^b (Å)^3
$Li_4MgIn_2F_{12}$	4.7286(6)	17.544(3)	5.0380(6)	104.4(2)
$Li_4FeIn_2F_{12}$	4.741(1)	17.573(6)	5.070(1)	105.6(3)
$Li_4CoIn_2F_{12}$	4.7472(6)	17.621(3)	5.0653(6)	105.9(2)
$Li_4NiIn_2F_{12}$	4.7350(6)	17.591(2)	5.0364(6)	104.9(2)
$Li_4ZnIn_2F_{12}$	4.7465(6)	17.592(2)	5.0582(6)	105.6(2)
$LiZnInF_6$	8.74_0	8.74_0	4.69_5	103.4

[a] From powder data.
[b] Cell volume/Z for $AMM'F_6$ formulation.

TABLE III

ATOMIC PARAMETERS, ANISOTROPIC TEMPERATURE FACTORS[a] $U_{ij} \times 10^4$ AND B_{eq} (Å^2) FOR $Li_4ZnIn_2F_{12}$

Atom	Site	x	y	z	U_{11}	U_{22}	U_{33}	U_{23}	U_{13}	U_{12}	B_{eq}
In	4c	0	0.1176(1)	$\frac{1}{4}$	118(1)	85(1)	88(1)	0	6(4)	0	0.77(1)
Zn-Li_1	4c	0	0.4516(1)	$\frac{1}{4}$	94(3)	148(3)	99(3)	0	−12(14)	0	0.90(2)
Li_2	4c	0	0.2953(6)	$\frac{1}{4}$	278(18)	—	—	—	—	—	2.19(14)
Li_3[b]	4c	0	0.7751(9)	$\frac{1}{4}$	177(27)	—	—	—	—	—	1.40(21)
F_1	8d	0.2361(4)	0.4616(1)	0.5794(4)	134(7)	142(7)	124(7)	2(6)	−19(8)	44(7)	1.05(5)
F_2	8d	0.2438(4)	0.6260(1)	0.5805(5)	163(9)	134(7)	143(9)	0(6)	52(9)	10(7)	1.16(6)
F_3	8d	0.2825(3)	0.2929(1)	0.5733(5)	161(8)	113(7)	209(9)	−52(8)	3(8)	−17(7)	1.27(6)

Note. Standard deviations are given in parentheses.

[a] The vibrational coefficient relates to the expression

$$T = \exp[-2\pi^2(h^2a^{*2}U_{11} + k^2b^{*2}U_{22} + l^2c^{*2}U_{33} + 2hka^*b^*U_{12} + 2hla^*c^*U_{13} + 2klb^*c^*U_{23}].$$

[b] This position is half occupied.

grams. Atomic scattering factors and anomalous dispersion corrections were taken from the International Tables for X-ray Crystallography (*19*). The intensities were corrected for Lorentz and polarization effects as well as for absorption. The use of the heavy atom method first made it possible to locate the indium atom in a 4*c* site. The corresponding refinement led to a reliability factor of $R = 0.31$. After successive difference Fourier maps and refinements we located the following atoms: one zinc (4*c* site), three fluorines (8*d* site), and two lithiums, Li2 and Li3 (4*c* site). The corresponding R value was 0.09. At this stage the current formulation was not balanced: "$Li_8Zn_4In_4F_{24}$" had an excess of cationic charges. After associating this result to the large isotropic thermal motions (u) of Zn^{2+} and Li_3^+ cations ($u_{Zn} = 0.036$, $u_{Li3} = 2.0$), we decided to check their two occupation rates (τ). In the next refinement, the reliability factor immediately dropped to $R = 0.03$, with the following values: $\tau_{Zn} = 0.26$ (instead of 0.5), $u_{Zn} = 0.01$, $\tau_{Li3} = 0.36$, $u_{Li3} = 0.45$. This was a proof of a half occupation rate for the zinc site, and of a partial occupation of the Li3 site. When anisotropic thermal motions were applied to all atoms except Li2 and Li3 with $\tau_{Zn} = 0.25$, the reliability factor fell to $R = 0.018$ and τ_{Li3} became 0.38 (with $u_{Li3} = 0.049$). As the Fourier difference map clearly showed a lack of electron density at the zinc position, we decided to fill this site with lithium (Li1). This implied the setting of the occupation rate of the Li3 position to $\tau = 0.25$ and led to a balanced formulation: $(Li2)_4(Li3)_2(ZnLi1)_2(In)_4F_{24}$ ($Li_4ZnIn_2F_{12}$, $Z = 2$). In these conditions, the last refinement using a weighting scheme and anisotropic thermal motions (except for Li2 and Li3) led to $R = 0.015$ and $R_w = 0.018$ (with $u_{Li3} = 0.0177$).

Further tests on occupation rates concerning Li1 and Li3 sites did not improve this final result. Table III lists the atomic coordinates and thermal parameters, and Table IV the main interatomic distances and angles. A table giving the calculated and observed structure factors may be obtained on request to the authors.

Structure Description and Discussion

The structure of $Li_4ZnIn_2F_{12}$ exhibits a new cationic distribution in an h.c. packing of F^- ions. Figure 1 shows a perspective view of the structure; it is built up by almost

TABLE IV

MAIN INTERATOMIC DISTANCES (Å) AND ANGLES (°) IN $Li_4ZnIn_2F_{12}$

			In^{3+} Octahedron			
In	F_1	F_1	F_2	F_2	F_3	F_3
F_1	**2.064(2)**	3.044(3)	3.023(2)	2.969(3)	2.978(2)	4.140(1)
F_1	95.0(0.1)	**2.064(2)**	2.969(3)	3.023(2)	4.140(1)	2.978(2)
F_2	93.8(0.1)	91.7(0.1)	**2.074(2)**	4.137(4)	2.776(2)	2.943(3)
F_2	91.7(0.1)	93.8(0.1)	171.8(0.1)	**2.074(2)**	2.943(3)	2.776(2)
F_3	91.7(0.1)	172.1(0.1)	83.7(0.1)	90.1(0.1)	**2.086(1)**	2.733(3)
F_3	172.1(0.1)	91.7(0.1)	90.1(0.1)	83.7(0.1)	81.9(0.1)	**2.086(1)**
			⟨In–F⟩ = 2.08 Å		d_{Shannon} = 2.10 Å	
			$(Zn^{2+}Li_1^+)$ Octahedron			
$ZnLi_1$	F_2	F_2	F_1	F_1	F_1	F_1
F_2	**1.986(2)**	2.882(3)	2.959(3)	2.869(2)	4.066(2)	2.895(2)
F_2	93.1(0.1)	**1.986(2)**	2.869(2)	2.959(3)	2.895(2)	4.066(2)
F_1	95.3(0.1)	91.6(0.1)	**2.017(2)**	4.019(3)	2.739(2)	2.869(3)
F_1	91.6(0.1)	95.3(0.1)	170.0(0.1)	**2.017(2)**	2.869(3)	2.739(2)
F_1	176.2(0.1)	90.7(0.1)	83.8(0.1)	88.8(0.1)	**2.083(2)**	2.831(3)
F_1	90.7(0.1)	176.2(0.1)	88.8(0.1)	83.8(0.1)	85.6(0.1)	**2.083(2)**
			⟨(ZnLi)–F⟩ = 2.03 Å		d_{Shannon} = 2.05 Å	
			Li_2^+ Octahedron			
Li_2	F_2	F_2	F_3	F_3	F_3	F_3
F_2	**1.999(7)**	2.882(3)	4.063(1)	2.941(2)	2.982(2)	2.880(3)
F_2	92.3(0.5)	**1.999(7)**	2.941(2)	4.063(1)	2.880(2)	2.982(2)
F_3	174.4(0.4)	92.6(0.1)	**2.068(8)**	2.733(3)	2.963(3)	2.911(2)
F_3	92.6(0.1)	174.4(0.4)	82.7(0.4)	**2.068(8)**	2.911(2)	2.963(3)
F_3	92.8(0.3)	88.8(0.2)	90.2(0.2)	88.1(0.3)	**2.117(2)**	4.232(3)
F_3	88.8(0.2)	92.8(0.3)	88.1(0.3)	90.2(0.2)	177.7(0.6)	**2.117(2)**
			⟨Li_2–F⟩ = 2.06 Å		d_{Shannon} = 2.06 Å	
			Li_3^+ Octahedron			
Li_3	F_3	F_3	F_3	F_3	F_2	F_2
F_3	**1.960(3)**	3.870(3)	2.963(3)	2.911(2)	2.880(3)	2.776(2)
F_3	161.6(0.9)	**1.960(3)**	2.911(2)	2.963(3)	2.776(2)	2.880(3)
F_3	96.6(0.3)	94.3(0.3)	**2.008(10)**	3.225(3)	2.941(2)	4.272(2)
F_3	94.3(0.3)	96.6(0.3)	106.8(0.7)	**2.008(10)**	4.272(2)	2.941(2)
F_2	84.9(0.4)	81.1(0.4)	86.1(0.2)	167.1(0.6)	**2.291(12)**	2.978(3)
F_2	81.1(0.4)	84.9(0.4)	167.1(0.6)	86.1(0.2)	81.1(0.5)	**2.291(12)**
			⟨Li_3–F⟩ = 2.09 Å		d_{Shannon} = 2.06 Å	

regular MF_6 octahedra. The Li3 octahedra, which belong to a half occupied site (see Table IV), are the most distorted. It must be borne in mind that only two of the three other cationic sites are occupied by a single kind of ion (In and Li2 sites), the last position being statistically filled by zinc and lithium. Nevertheless, it is clear that the cell parameters as well as the space group (*Pbcn*) are typical for a tri-α-PbO_2 structure, such as Fe_2WO_6 (*14*), $ZnTa_2O_6$ (*20*), or LiSb WO_6 (*21*).

From a crystal chemical point of view, some features of the tri-α-PbO_2 structure can be recognized in $Li_4ZnIn_2F_{12}$ (see the (100) projections given in Fig. 2 for levels $x = 0$ and $x = \frac{1}{2}$). The main feature of the tri-α-PbO_2 structure-type consists of zigzag chains of edge sharing octahedra parallel to the *c* axis. A specific order between these

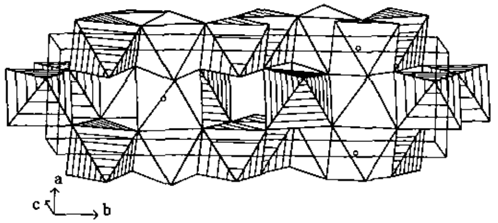

FIG. 1. Perspective view of $Li_4ZnIn_2F_{12}$ structure (*23*). In octahedra are strongly shaded, whereas (Zn/Li) ones are lightly shaded. Li2 and Li3 octahedra are unshaded. Circles correspond to Li3 atom (half occupation rate).

chains is responsible for the threefold increase of the *b* axis; for example the sequence Li–Li/W–Sb/Sb–W/Li–Li is observed for $LiSbWO_6$ (Fig. 1, right part). The same ordered zigzag chains are evidenced for $Li_4ZnIn_2F_{12}$ if the Li2 site is overshadowed (Fig. 1, left part), the remaining difference being the half occupied Li3 position.

In our case, the occupation ratio for the octahedral sites, 0.583 instead of 0.50 for $AMM'X_6$ compounds, leads to some modifications in the cationic distribution and in the connections between the octahedra. Indeed Li2 and Li3 octahedra share not only edges in the *c* direction, but also faces in the *a* direction. These connections lead to the presence of corrugated (*a*, *c*) planes at $y \approx 0.29$ and 0.77, as illustrated in Fig. 3. In these never-ending planes, 75% of the octahedral sites are occupied.

It is surprising to note that no $AMM'F_6$ compound with a tri-α-PbO_2 structure has been reported. The same remark was made in the past by Senegas and Galy (*22*) for fluorinated phases which never crystallize with the columbite structure. From a geometrical point of view, these two structures could exist, but electrostatic effects seem to be predominant and the stabilization is therefore prevented. Indeed, in the case of "$LiZnInF_6$" with the tri-α-PbO_2 structure type, the sharing of edges between In and Zn octahedra in the zigzag chains would not be favored by Pauling's rules, which state that polyhedra around the more charged cations tend not to share edges and especially

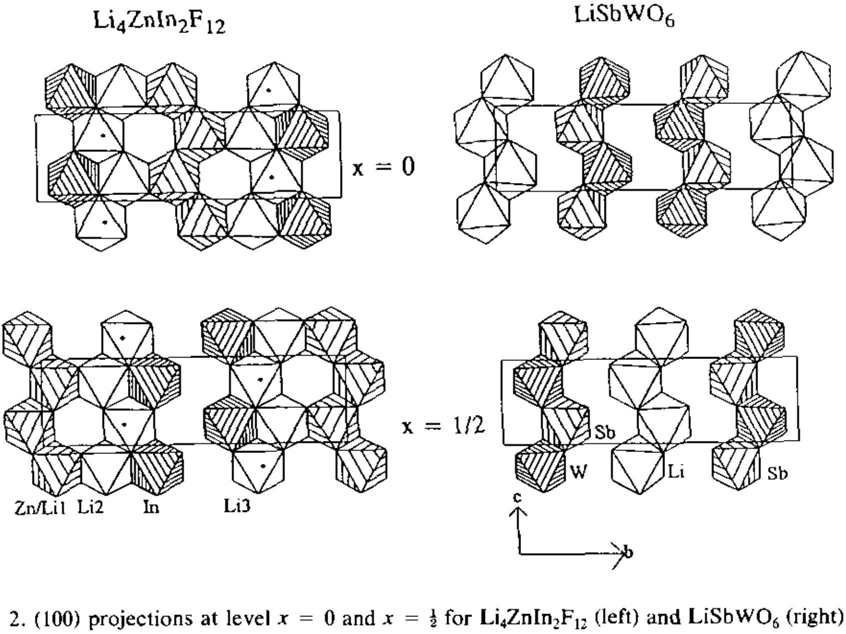

FIG. 2. (100) projections at level $x = 0$ and $x = \frac{1}{2}$ for $Li_4ZnIn_2F_{12}$ (left) and $LiSbWO_6$ (right).

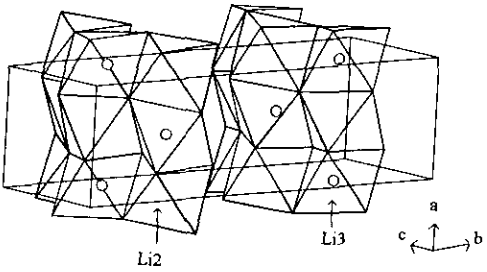

FIG. 3. Corrugated planes of lithium octahedra in $Li_4ZnIn_2F_{12}$.

faces, but vertices. In agreement with these rules, the cationic distribution of $Li_4ZnIn_2F_{12}$ is preferred, because the indium octahedra do not share edges with the zinc/lithium ones; only three edges are shared with the lithium octahedra, two of them being half occupied. Moreover, the octahedra face sharing is only encountered for the less charged cations.

Conclusion

The $Li_4MIn_2F_{12}$ phases manifest a new cationic distribution inside an h.c. packing of F^- ions. The stacking of octahedra is strongly related to the tri-α-PbO_2 structure, which has never been observed for fluorinated compounds.

At the present time, the occupation of additional octahedral sites ($\tau = 0.583$ instead of 0.5) seems to be the only way to obtain such a structure type (F^- network). This could be the explanation for the absence of structural transition between Na_2SiF_6 (or Trirutile) and tri-α-PbO_2 types for $AMM'F_6$ compounds.

Acknowledgments

The authors are grateful to Dr. R. Retoux for his help in X-ray data collection, and to Dr. L. Permer for her critical reading.

References

1. R. M. Metzger, N. E. Heimer, C. S. Kuo, R. F. Williamson, and W. O. J. Boo, *Inorg. Chem.* **22,** 1060 (1983).
2. W. Viebahn and P. Epple, *Z. Anorg. Allg. Chem.* **427,** 45 (1976).
3. J. Portier, F. Menil, and A. Tressaud, *Mater. Res. Bull.* **5,** 503 (1970).
4. J. Portier, A. Tressaud, R. de Pape, and P. Hagenmuller, *C. R. Acad. Sci. Paris Ser. C* **267,** 1711 (1968).
5. D. Babel and A. Tressaud, *in* "Inorganic Solid Fluorides" (P. Hagenmuller, Ed.), p. 77, Academic Press, New York (1985).
6. W. Viebahn, *Z. Anorg. Allg. Chem.* **413,** 77 (1975).
7. G. Courbion, C. Jacoboni, and R. de Pape, *Acta Crystallogr.* **633,** 1405 (1977).
8. G. Courbion, C. Jacoboni, and R. de Pape, *J. Solid State Chem.* **45,** 127 (1982).
9. J. Gaile, W. Rudorff, and W. Viebahn, *Z. Anorg. Allg. Chem.* **430,** 161 (1977).
10. F. Menil, J. Grannec, G. Demazeau, and A. Tressaud, *C. R. Acad. Sci. Paris Ser. C* **275,** 495 (1972).
11. T. Sekino, T. Endo, T. Sato, and M. Shimada, *J. Solid State Chem.* **88,** 505 (1990).
12. G. Courbion, C. Jacoboni, and P. Wolfers, *Eur. J. Solid State Inorg. Chem.* **25,** 359 (1988).
13. N. Halle and H. K. Müller-Buschbaum, *J. Less-Common Met.* **142,** 263 (1988).
14. J. Senegas and J. Galy, *J. Solid State Chem.* **10,** 5 (1974).
15. J. Nouet, C. Jacoboni, G. Ferey, J. Y. Gerard, and R. de Pape, *J. Cryst. Growth* **47,** 699 (1979).
16. G. Courbion, Thesis, Le Mans (1979).
17. G. M. Sheldrick, "SHELX76, A Program for Crystal Structure Determination," Cambridge Univ. Press, London/New York (1976).
18. "Cristallographic Computing 3" (G. M. Sheldrick, C. Krüger, and R. Goddard, Eds.), p. 175, Oxford Univ. Press, London/New York (1985).
19. "International Tables for X-ray Crystallography," Vol. IV, Kynoch, Birmingham (1968).
20. M. Waburg and H. K. Müller-Buschbaum, *Z. Anorg. Allg. Chem.* **508,** 55 (1984).
21. A. Le Bail, H. Duroy, and J. L. Fourquet, *Mater. Res. Bull.* **23,** 447 (1988).
22. J. Senegas and J. Galy, *J. Solid State Chem.* **5,** 481 (1972).
23. R. X. Fisher, *J. Appl. Crystallogr.* **18,** 258 (1985).